Journal of Colloid and Interface Science 357 (2011) 82–87

Contents lists available at ScienceDirect

Journal of Colloid and Interface Science

www.elsevier.com/locate/jcis

Scattering of intersecting spherical particles in the Rayleigh-Gans approximation

Guillermo E. Eliçabe *

Institute of Materials Science and Technology (INTEMA), University of Mar del Plata and National Research Council (CONICET), J.B. Justo 4302, 7600 Mar del Plata, Argentina

ARTICLE INFO

Article history:
Received 23 November 2010
Accepted 22 January 2011
Available online 1 February 2011

Keywords:
Scattering
Colloids
Pickering emulsions
Lock and key colloids
Janus particles

ABSTRACT

In this work a novel semianalytical procedure to calculate the exact scattering behavior of complex particles made of intersecting spheres in the Rayleigh-Gans approximation is presented. Pickering emulsions, Janus particles, and lock and key particle colloids are particular cases of particles built from intersecting spheres. The proposed methodology is based on the decomposition of the complex particle as a sum of simpler components whose scattering properties can be evaluated using a simple integral. The procedure is developed for any number of spheres that intersect in pairs but it can be directly extended to intersections that involve more than two spheres at the same time. Some examples are presented to illustrate the application of the model to: (i) the study of the sensitivity of scattering spectra to detect complex particles from approximated model particles; (ii) the detection of different degrees of penetration of one particle into the other; (iii) the identification of the location of the cavity in particles that intersect with a spherical surface of contact; and (iv) the follow up of the evolution of a complex particle from a mix of its components.

1. Introduction

Interest in colloidal inhomogeneous particles with complex shapes has increased considerably due to their potential applications in multiple areas of materials science [1]. This type of particle can be used as attractive building blocks to create materials with extraordinary properties to be applied in chemistry, applied optics, or biology. For instance, anisotropic colloidal particles have been shown to be very useful for controlling molecular recognition and self-assembling processes, which are subjects of current interest in materials science. Also, complex colloidal particles with controlled surface structures have been used extensively in studies of controlled formation of hierarchically structured materials due to the wide range of sizes and materials accessible using these particles [2].

Spherical particles are in most cases the building blocks of these complex colloids. These particles are many times organized as a group of intersecting spheres that structure the complex colloidal unit. The number of spheres in this unit may vary from a couple to a many of them. Also many times, the spheres that form the complex colloid are made of different materials and for that reason the type of intersection noted before depends on the application and must be specified. Fig. 1 shows cross sections of two intersecting spheres with different kinds of contact surfaces between them. For instance, Pickering emulsions [3] are colloidal systems in which a large spherical particle is stabilized by the addition of a large number of small ones incrusted on its surface. In this case the spheres intersect in a form such that the small ones occupy the intersecting volume and the large one is deformed to accept the small ones in it, which corresponds to the intersecting spheres of Fig. 1a. Janus particles [4] are another type of colloidal particles that can be thought as a group of intersecting spheres. This is possible when the asymmetry is only due to the surface chemical groups, as well as when biphasic particles such as bicompartmental particles are considered. In this last case, the type of intersection present in the particle is as in Fig. 1b. Recently, colloidal systems that have attracted interest are the ones that follow the lock and key principle [5], in which colloidal spheres as keys and monodisperse colloidal particles with a spherical cavity as locks bind spontaneously and reversibly via the depletion interaction. The morphology of these complex colloidal particles presents intersections also of the type shown in Fig. 1a. Other complex particles that can be described as intersections of spherical ones are dumbbell, snowman, and raspberry particles [2,6–8].

The study of the scattering characteristics of complex colloidal particles is an important topic related to the morphological characterization of the particles and to the understanding of their optical functional behavior. Exact scattering models of complex particles have become available in the last few years [9]. However, these models are difficult to implement and require, in general, lengthy computations. A widely used alternative to the exact model is the Rayleigh-Gans (RG) approximation [10]. This approximation is valid for particles that present a low optical contrast with respect to the ambient medium, and are also sufficiently small so that the

* Fax: +54 223 481 0046.
E-mail address: elicabe@fi.mdp.edu.ar

0021-9797/$ - see front matter © 2011 Elsevier Inc. All rights reserved.
doi:10.1016/j.jcis.2011.01.077

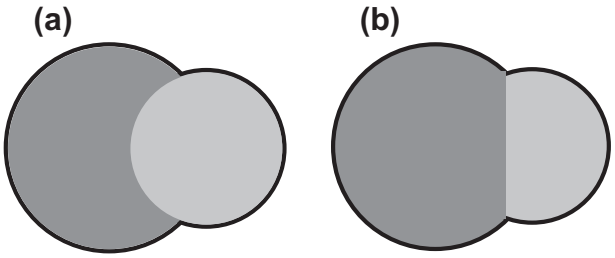

Fig. 1. Cross sections of possible spherical particle–spherical particle intersections: (a) spherical surface of contact between the two spheres; (b) plane surface of contact between the two spheres.

phase shift between incident and scattered light is also small. The conditions of validity for the RG approximation are always fulfilled in X-ray scattering but are more difficult to accomplish in light scattering.

A large variety of complex particles have been modeled in the RG approximation. However, scattering studies of the type of particles described in the previous paragraphs are more limited. For instance, the scattering of Pickering emulsions has been studied very recently using a simplified version of the RG theory [11]. Exact solutions of the RG theory have been obtained for different types of Janus particles [12,13]. These latter results involve the numerical evaluation of integrals of relatively complex functions. However, there is no general methodology available in the literature for calculating exactly the scattering properties of an arbitrary group of intersecting spheres in the RG approximation.

In this work a rather general procedure to calculate the exact scattering behavior of complex particles made of intersecting spheres in the RG approximation is presented. Pickering emulsions, Janus particles, and lock and key particle colloids are particular cases of particles built from intersecting spheres. The proposed methodology is based on the decomposition of the studied particle into a group of particles in which the scattering properties of the individual units can be evaluated using a simple integral, as done when spherical symmetry exists. The procedure is developed for a group of spheres that intersect as in Fig. 1a and it can be directly used to model Pickering emulsions, lock and key particle colloids, snowman particles, and others.

2. Theory

A group of N arbitrary scattering units located at positions given by $\mathbf{R}j$ ($j = 1, \ldots, N$) scatters incident monochromatic light with amplitude electric field, E_S, given by [14]

$$E_S(\mathbf{a}) = -E_0 \frac{\exp(ika)}{a} \sum_{j=1}^{N} b_j(\mathbf{q}) \exp(-i\mathbf{q}\cdot\mathbf{R}_j), \tag{1}$$

where vector $\mathbf{a}$ ($|\mathbf{a}| = a$) indicates the position of the detector, E_0 is the magnitude of the incident field which in this case is assumed to be polarized perpendicular to the scattering plane, $\mathbf{q} = \mathbf{q}_s - \mathbf{q}_i$ is the scattering vector ($|\mathbf{q}| = q = \frac{4\pi}{\lambda}\sin 1/2\theta$), $\mathbf{q}_i$ and $\mathbf{q}_s$ are the propagation vectors of the incident and scattering fields, respectively, $k = 2\pi/\lambda$ is the magnitude of the propagation vector of the incident radiation, θ is the scattering angle, λ is the wavelength of the incident radiation in the medium, and b_j is the scattering length of scattering unit j. Note that time dependence has been omitted.

Assume that this group of N scattering units corresponds to a complex particle composed of intersecting spheres as, for instance, the Pickering-type particle shown in Fig. 2. In Fig. 3 a possible schematic decomposition of this particle is considered, in a fashion similar to that used in Ref. [15]. As seen, the intersections correspond

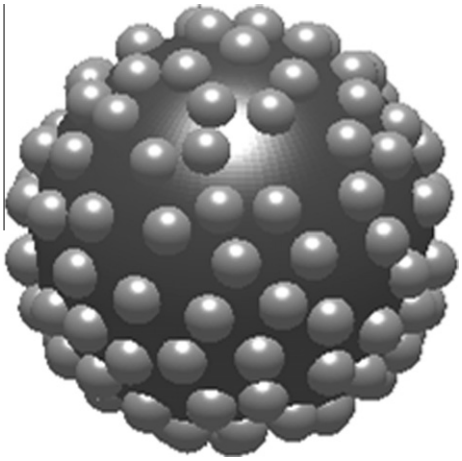

Fig. 2. Inhomogeneous Pickering-type particle composed of intersecting spheres used to develop the model.

to the type described in Fig. 1a. In this example the large sphere has a given contrast and the small ones are all of the same size and contrast, which is different than the contrast of the large sphere.

According to Fig. 3, the amplitude electric field can now be written as

$$E_S(\mathbf{a}) = -E_0 \frac{\exp(ika)}{a}\left[\sum_{j=1}^{N_i} b_{R_j^*}(\mathbf{q}) + b_r(\mathbf{q})\sum_{j=1}^{N_i}\exp(-i\mathbf{q}\cdot\mathbf{R}_j) - (N_i - 1)b_R(\mathbf{q})\right], \tag{2}$$

where $N_i = N - 1$ is the number of small spheres and the scattering lengths of the large and small spheres are given by [10]

$$b_R(\mathbf{q}) = \Delta\rho_1 V_R F(q, R), \tag{3}$$

$$b_r(\mathbf{q}) = \Delta\rho_2 V_r F(q, r), \tag{4}$$

with

$$F(q, x) = \left[\frac{3}{(qx)^3}(\sin qx - qx\cos qx)\right]. \tag{5}$$

Here, $\Delta\rho_1$ and $\Delta\rho_2$ are the contrast scattering length densities (CSLDs) of the large and small spheres, respectively; R is the radius of the large sphere; r is the radius of the small spheres; $V_R = \frac{4}{3}\pi R^3$; and $V_r = \frac{4}{3}\pi r^3$.

Finally, following the decomposition of Fig. 3c, the $b_{R_j^*}(\mathbf{q})$'s ($j = 1, \ldots, N_i$) are the scattering lengths of N_i irregular particles, with each one a spherical particle of the same size and contrast as the large sphere, with a spherical cavity in one of the different N_i positions where the intersecting small spheres are localized. If the plane z–y is taken as the scattering plane, the expression for the scattering length of these particles is [10]

$$b_{R_j^*}(\mathbf{q}) = \Delta\rho_1 \int_{-R}^{R} \exp(i2k\xi\sin\theta/2) A_j(\theta, \xi) d\xi, \quad j = 1, \ldots, N_i, \tag{6}$$

where ξ is the perpendicular distance from the origin of coordinates to intersecting planes which are perpendicular to vector $\mathbf{q}$, and $A_j(\theta, \xi)$ is the area of the intersection of those intersecting planes with the volume of the j sphere with spherical cavity, for a given value of ξ and θ. This area, which for the case of a simple sphere is independent of θ and is given by $A(\xi) = \pi(R^2 - \xi^2)$, cannot be expressed as a simple function for the sphere with spherical cavity.

With the purpose of computing the $A_j(\theta, \xi)$'s for all the spheres with spherical cavity, all possible intersections of the "intersecting planes" with a generic sphere with spherical cavity must be

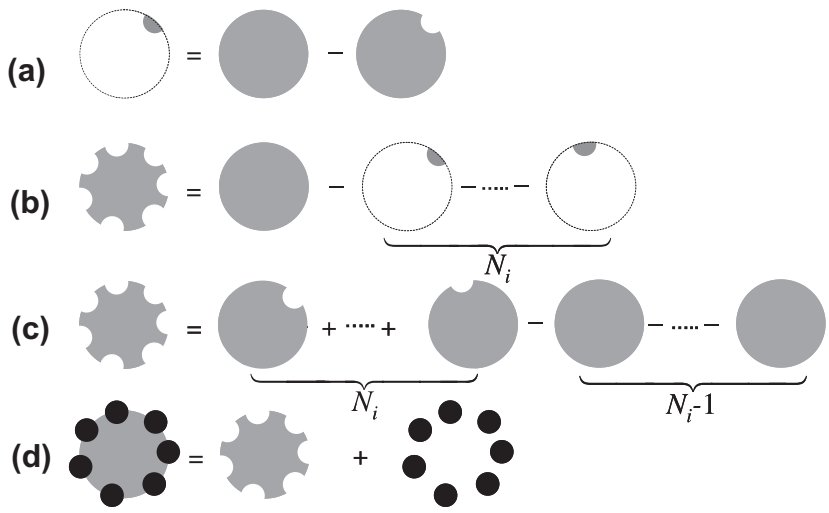

Fig. 3. Decomposition of a complex particle, represented by several small spheres incrusted on the surface of a large one, into a sum of simpler components.

considered. First, in order to simplify the notation, subscript j is dropped from $A_j(\theta,\xi)$. Assume now, to help with the analysis, that there are two mutually overlapping spheres of radii R and r, in the same positions as the sphere with spherical cavity and a hypothetical sphere that perfectly fits in the spherical cavity, respectively. Thus, the result of the intersection of the intersecting plane and the two mutually overlapping spheres is a pair of circles of radii R' and r', corresponding to the intersections with the spheres of radii R and r, respectively. It is assumed here that the intersecting plane intersects both spheres. If only the sphere with spherical cavity is intersected, then $A(\theta,\xi)=\pi R'^2$. In Fig. 4 this pair of circles is depicted for all of their relative sizes and positions. In that figure, three variables and a function are defined: (i) r' is the radius of the intersected circle on the sphere of radius r; (ii) R' is the radius of the intersected circle on the sphere of radius R; (iii) d' is the distance between the centers of the intersected circles; and (iv) $A^*(\theta,\xi)$ is the area of the intersection of the areas of both circles in cases a.2 and b.2. It can be easily verified that the value of $A(\theta,\xi)$, which is the variable that must be calculated, is the difference between the area of the circle of radius R' and the area of the intersection between the areas of the circles of radii R' and r'. At the bottom of each subfigure of Fig. 4 the values of $A(\theta,\xi)$ are also given. Note that in case b.3 $A(\theta,\xi)=0$ because $R'<r'$. $A(\theta,\xi)$, which represents the area of the intersection of the intersecting plane with the volume of the sphere with spherical cavity, corresponds to the shaded areas shown in Fig. 4 for each case.

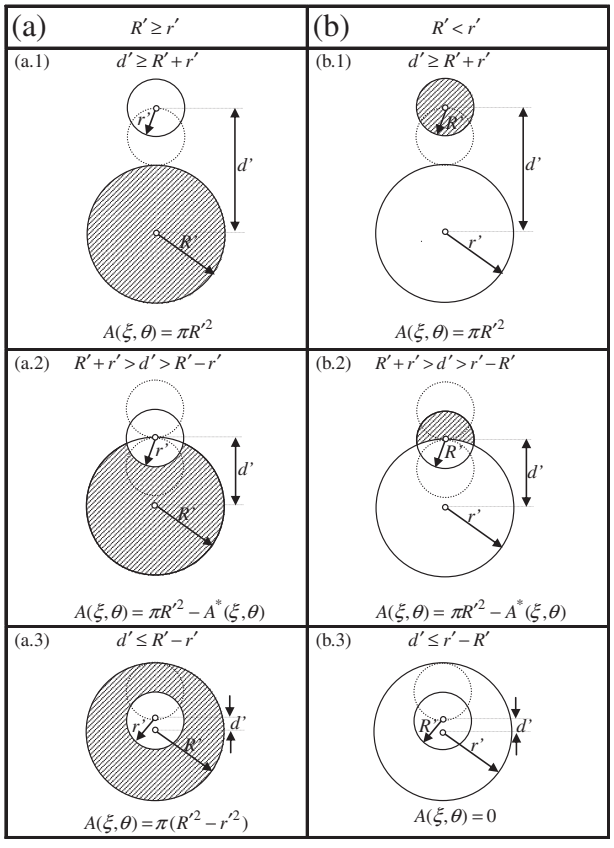

Fig. 4. Pair of circles representing all possible kinds of intersections of the intersecting plane and the two mutually overlapping spheres of radii R and r. The shaded areas represent the values of $A(\theta,\xi)$, given at the bottom of each of the subfigures. The dotted circles correspond to the limiting values of d'.

In order to clarify how the values of R', r', and d' are calculated, in Fig. 5 a schematic representation of the two mutually overlapping spheres of radii R and r corresponding to the case of Fig. 4a.2 is considered. The resulting two-dimensional representation of this intersection helps to understand how, using simple geometry, the values of R', r', d', and $A^*(\theta,\xi)$ can be calculated in the following way

$$R' = \sqrt{R^2 - \xi^2} \tag{7}$$

$$r' = [r^2 - (\xi - y_0\cos\theta/2 + z_0\sin\theta/2)^2]^{1/2} \tag{8}$$

$$d' = [(z_0\cos\theta/2 + y_0\sin\theta/2)^2 + x_0^2]^{1/2} \tag{9}$$

$$A^*(\xi,\theta) = r'^2\cos^{-1}\left(\frac{d'^2+r'^2-R'^2}{2d'r'}\right) + R'^2\cos^{-1}\left(\frac{d'^2+R'^2-r'^2}{2d'R'}\right)\cdots - \frac{1}{2}\left[(-d'+r'+R')(d'+r'-R')(d'-r'+R')(d'+r'+R')\right]^{1/2}, \tag{10}$$

where (x_0, y_0, z_0) are the coordinates of the center of the sphere of radius r.

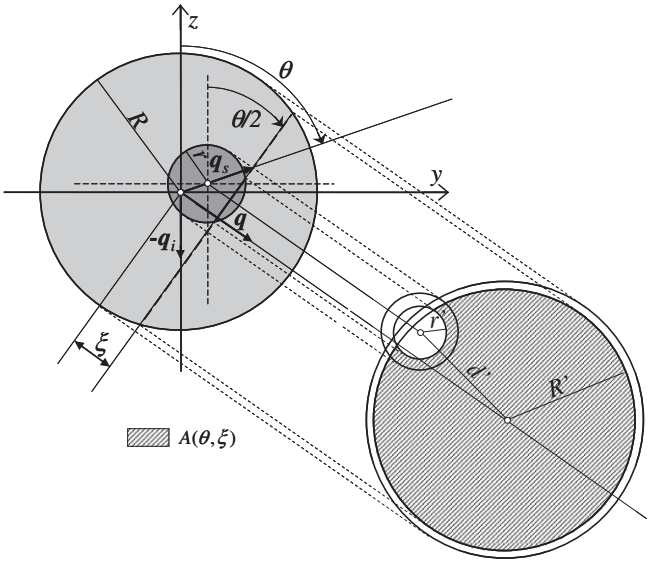

Fig. 5. Schematic representation of the two mutually overlapping spheres of radii R and r corresponding to the case of Fig. 4a.2. The left part represents the pair of mutually overlapping spheres as seen from the positive x direction. The right part represents the intersection of a plane perpendicular to plane z–y and to vector $\mathbf{q}$, located at a distance ξ from the origin, with the pair of the left part of the figure.

In order to compute the scattering length of the spheres with spherical cavity the integral of Eq. (6) must evaluated numerically. According to Fig. 4 the value of $A(\theta,\xi)$, for a given θ and ξ, is calculated as shown in the logical diagram of Fig. 6, where the first question to answer is if the small sphere defining the spherical cavity is intersected by the intersecting plane.

The quantity usually measured in scattering experiments is the differential scattering cross section (DSCS), which for the studied particle in fixed position is given by

$$\frac{d\sigma(q)}{d\Omega}=\frac{|E_S(\mathbf{a})|^2a^2}{E_0^2}=\left|\sum_{j=1}^{N_i}b_{R'_j}(\mathbf{q})+b_r(\mathbf{q})\sum_{j=1}^{N_i}\exp(-i\mathbf{q}\cdot\mathbf{R}_j)-(N_i-1)b_R(\mathbf{q})\right|^2. \tag{11}$$

3. Simulated results

In this section the previous theoretical results will be used to generate the average differential scattering cross section (ADSCS) spectra of different complex particles. The simulations are intended to verify, first, the sensitivity of the spectra to recognize these complex particles, by means of comparing the spectra with those of commonly used approximations to the complex particles, such as core–shell particles. Also the sensitivity of the spectra to variations into some of the parameters describing the morphology of the particles will be verified.

First, and in order to check the validity of the proposed methodology, the spectrum of a sphere with spherical cavity is calculated using not only the method described here but also Monte Carlo simulation. The sphere with spherical cavity is an adequate testing particle in order to verify the proposed methodology because together with the sphere they are the blocks used to build all the other particles made of intersecting spheres. For this simulation a sphere of radius $R = 10$ nm with a spherical cavity of radius $r = 8$ nm is used. The distance between the centers of both spheres is equal to 10 nm. The q range selected (10^{-3} to 1 nm^{-1}) corresponds, for instance, to an angular range from 0.001824° to 1.839° for X-rays of wavelength $\lambda = 0.2$ nm. The Monte Carlo simulation is performed using the method proposed in Ref. [15], in which the pair distribution function, $P(r)$, can be calculated after filling the particle with a large number of randomly located coordinate points and counting all the distances between them. Then, the ADSCS is calculated using

$$\left\langle\frac{d\sigma(q)}{d\Omega}\right\rangle=\frac{1}{4\pi}\int_0^D P(r)\frac{\sin(qr)}{qr}dr, \tag{12}$$

where D is the maximum distance between two points in the particle. In Fig. 7 the spectra calculated using the proposed methodology and Monte Carlo simulation, are shown. As expected both calculations coincide at a visual level, validating the semianalytical method proposed here. The spectrum of a sphere of radius $R = 10$ nm is also included in Fig. 7 to show the effect of the cavity on the scattering characteristics of spherical particles with spherical cavities.

The next example corresponds to the Pickering-type particle shown in Fig. 2. This particle has $N_i = 120$ small spheres of radius

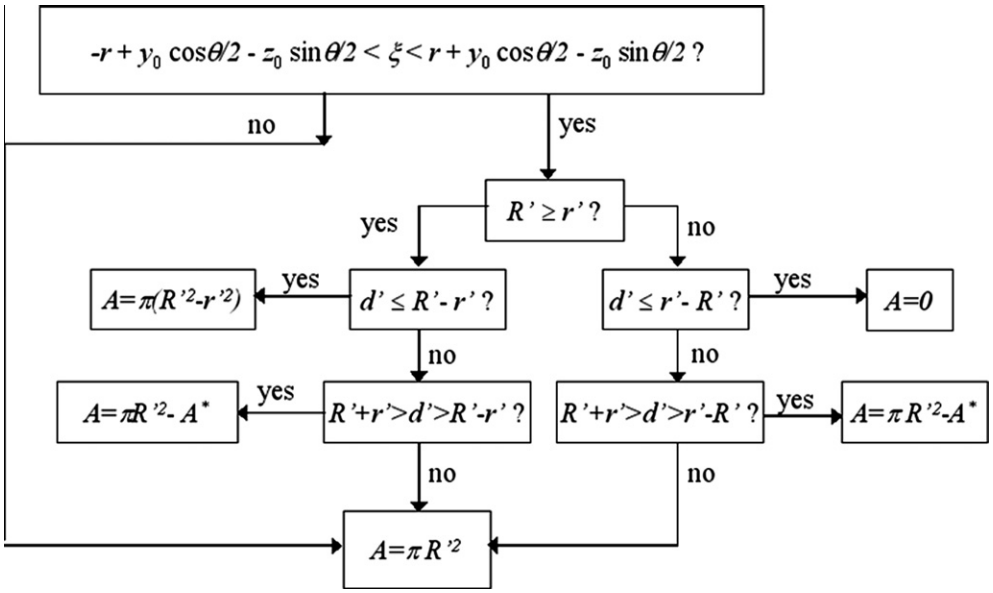

Fig. 6. Logical diagram used to calculate $A(\theta,\xi)$ for given values of ξ and θ, according to the different possibilities described in Fig. 4.

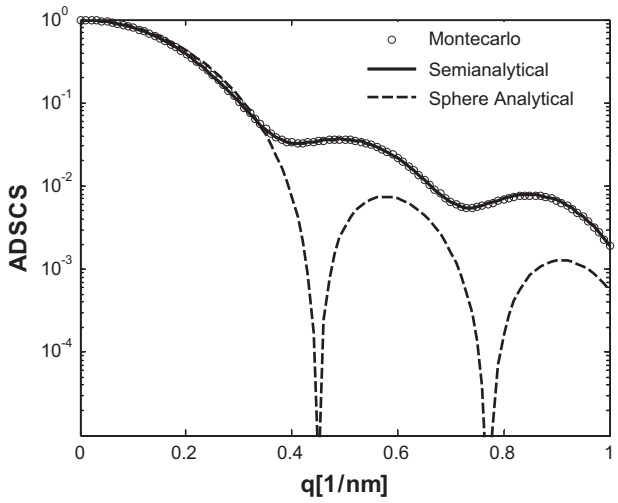

Fig. 7. ADSCSs of sphere with spherical cavity: Semianalytical (—) and Monte Carlo (ooooo); and sphere: Analytical (———).

$r = 4$ nm incrusted into a large sphere of radius $R = 31.3$ nm. The centers of the small spheres lay on the surface of the large one. The q range selected is the same as the previous example, 10^{-3} to 1 nm^{-1}. Two different ratios of the CSLDs of the particles were selected: $\Delta\rho_1/\Delta\rho_2 = 6$ and $\Delta\rho_1/\Delta\rho_2 = 1/6$. In order to compare with the Pickering-type particle, two other particles were considered. One is a core–shell particle with shell radius of 32.6 nm (CSLD $\Delta\rho_2$) and core radius of 30 nm (CSLD $\Delta\rho_1$). The other is a decorated particle, which is a cluster of spherical particles [16], that consist of a sphere of 30 nm of radius (CSLD $\Delta\rho_1$), decorated with $N_i = 120$ spheres of radius 4 nm (CSLD $\Delta\rho_2$) located on the surface of the large sphere. The dimensions of these two particles were selected so that the total material of CSLD $\Delta\rho_1$ and the total material of CSLD $\Delta\rho_2$, are the same as in the Pickering-type particle.

In Fig. 8 the DSCS spectra of these particles are shown for $\Delta\rho_1/\Delta\rho_2 = 6$ (Fig. 8a) and $\Delta\rho_1/\Delta\rho_2 = 1/6$ (Fig. 8b). The reported spectra of the Pickering-type and decorated particles are obtained, for each type of particle, by averaging the spectra of 100 different particles generated by randomly placing the small spheres with their centers on the interface of the large sphere and the surrounding medium, for the Pickering-type particle, and with their centers at a distance r from the surface of the large sphere, for the decorated particle.

As it can be seen, for both contrast ratios the oscillatory spectrum of the core–shell particle departs distinctively from that of the Pickering-type particle at high q values. This departure, which is related to the presence of the small spheres instead of a homogeneous shell, is similar for both contrasts. The example shows the sensitivity of the DSCS spectrum of the Pickering-type particle to distinguish it from a commonly used approximation, the core–shell particle.

A comparison of the spectra of the Pickering-type particle with those of the decorated particle allows one to check the sensitivity of the spectra of the Pickering-type particle with respect to the degree of penetration of the small spheres into the large one. Also in this case, the spectra of the Pickering-type particle show clear differences with respect to those of the decorated particle. For $\Delta\rho_1/\Delta\rho_2 = 6$, this is when the large sphere is dominant, the difference is important only at high q values. However, when the small spheres are dominant, $\Delta\rho_1/\Delta\rho_2 = 1/6$, the difference is more evident at low q.

In the following, lock and key particles made of only two intersecting spheres are considered. Two cases are analyzed with this configuration using the same range of q as in the previous example.

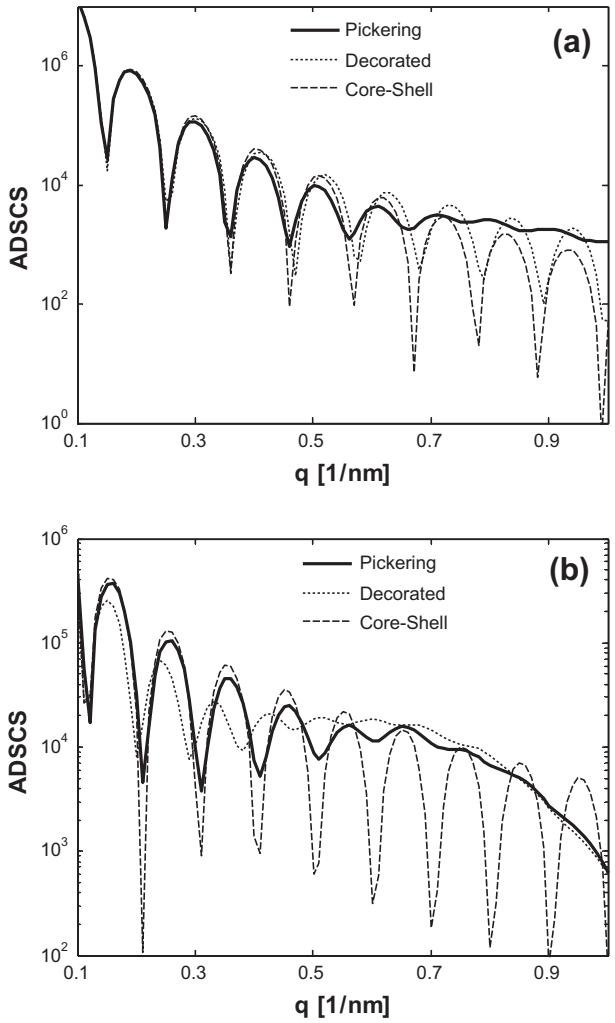

Fig. 8. ADSCSs of Pickering-type (—), decorated (……), and core–shell (———) particles: (a) for $\Delta\rho_1/\Delta\rho_2 = 6$ and (b) for $\Delta\rho_1/\Delta\rho_2 = 1/6$.

In the first case, the radii of the intersecting spheres are 16 and 30 nm. The spheres are considered to intersect in the two possible forms: the small one penetrating the large one and vice versa. In both cases the center of the small sphere lays on the surface of the large one. Also the same contrast ratios of the previous example are taken into account: $\Delta\rho_1/\Delta\rho_2 = 6$ and $\Delta\rho_1/\Delta\rho_2 = 1/6$. In Fig. 9, the spectra of these lock and key particles are shown in an arbitrary scale. It can be noted that when the large sphere has the smaller contrast there is a clear difference in the spectra between the case in which the spherical cavity is in the large sphere and the case in which it is in the small one. When contrast is reversed, the form in which the spheres intersect is hardly noticeable in the spectra. In this figure $\Delta\rho$ is the contrast between the gray particle and the surrounding medium.

In the second case the analysis is focused in detecting the sensitivity of the spectrum to discriminate between: (i) a mixture of lock and key particles made of two intersecting spheres, in random positions; and (ii) a mixture of: spheres with spherical cavity in random positions and simple spheres, which could conform the lock and key particles. In this case the CSLDs of the large and small spheres are taken to be the same, and their radii are taken as 30 and 22 nm. Again the small sphere lays on the surface of the large one. The two generated spectra are shown in Fig. 10.

The spectra are calculated by averaging the spectra of the anisotropic particles placed in 100 different randomly generated

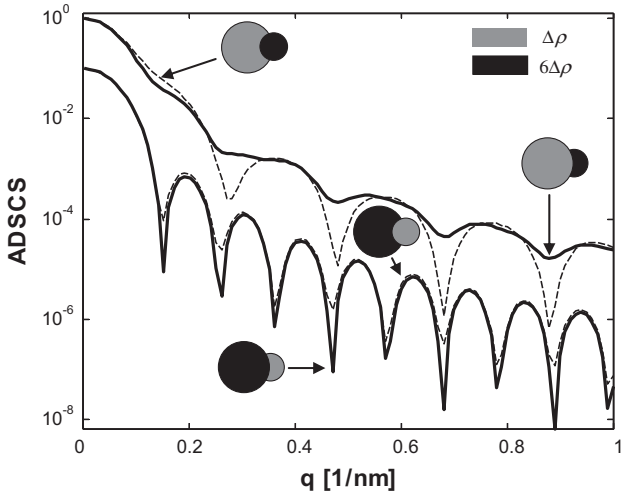

Fig. 9. ADSCSs of lock and key particles with $\Delta\rho_1 = 1/6\Delta\rho_2$ and $\Delta\rho_1 = 6\Delta\rho_2$: spherical cavity in the large sphere (———), and spherical cavity in the small sphere (—).

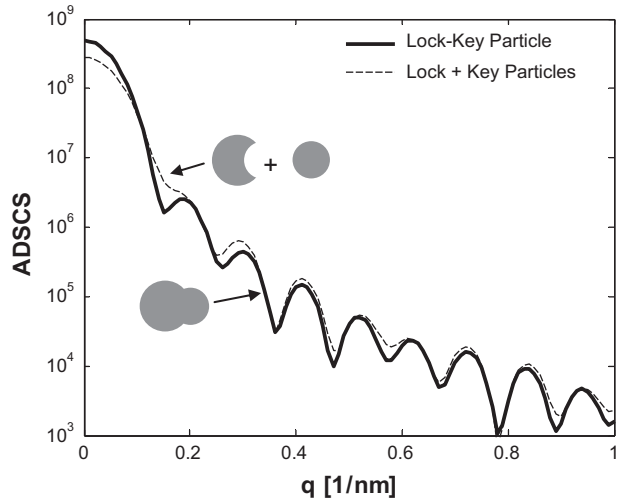

Fig. 10. ADSCSs of: lock and key particle (—), and mix of components of the lock and key particle (———).

orientations. In contrast to the previous examples in which the spectra are plotted in arbitrary relative scales, in this case the relative scales are preserved. In this form the two spectra can be visualized as the initial and final stages of a dynamic process of particle formation, which starts with a mixture of large spheres with spherical cavity and small spheres, and ends with the formation of lock and key particles as a result of the proper combination of the initial mixture components. A noticeable change in the spectrum of the lock and key particles with respect to that of a mix of the components of that particle can be appreciated in Fig. 10.

4. Conclusions

The semianalytical model presented here is completely general and allows one to generate a scattering spectrum of any combination of intersecting spheres composing a complex particle, for which the surface of contact between the spheres is spherical. The same methodology used to develop the model for spherical surface of contact can be applied to the case in which the surface of contact is not spherical. The key to the method is the decomposition of the complex particle as a sum of simpler components. In the case developed here two types of units compose the complex particle: the sphere and the sphere with spherical cavity. The method is not computationally expensive and then numerical orientational averaging is practically possible.

The examples presented show that scattering experiments could detect in some cases the type of complex particles described in this work from simpler structures usually taken as approximated models of the complex particles. In some cases it was possible to detect degree of penetration of one particle into the other, and, for particles externally equal, the location of the spherical cavity. It was also shown in a particular case that, starting from a mix of its components, it is possible to follow the evolution of a complex particle formation, through its scattering spectra.

As far as we know, the model presented here addresses for the first time in a rigorous manner the problem of computing the scattering properties of intersecting spheres in the RG approximation. The software used to implement the model discussed in this work is available from the author on request.

Acknowledgments

I acknowledge the financial support of the following institutions of Argentina: University of Mar del Plata, National Research Council (CONICET), and National Agency for the Promotion of Science and Technology (ANPCyT).

References

[1] A. Perro, S. Reculusa, E. Bourgeat-Lami, E. Duguet, S. Ravaine, Colloids Surf., A 284–285 (2006) 78.
[2] W.S. Choi, H.Y. Koob, W.T.S. Huck, J. Mater. Chem. 17 (2007) 4943.
[3] S.U. Pickering, J. Chem. Soc. 91 (1907) 2001.
[4] A. Perro, S. Reculusa, S. Ravaine, E. Bourgeat-Lamic, E. Duguet, J. Mater. Chem. 15 (2005) 3745.
[5] S. Sacanna, W.T.M. Irvine, P.M. Chaikin, D.J. Pine, Nature 464 (2010) 575.
[6] P.M. Johnson, C.M. van Kats, A. van Blaaderen, Langmuir 21 (2005) 11510.
[7] S. Reculusa, C. Poncet-Legrand, A. Perro, E. Duguet, E. Bourgeat-Lami, C. Mingotaud, S. Ravaine, Chem. Mater. 17 (2005) 3338.
[8] D. Nagao, C.M. van Kats, K. Hayasaka, M. Sugimoto, M. Konno, A. Imhof, A. van Blaaderen, Langmuir 26 (2010) 5208.
[9] A. Doicu, T. Wriedt, Y.A. Eremin, Light Scattering by Systems of Particles. Null-Field Method with Discrete Sources: Theory and Programs, Springer Series in Optical Sciences, vol. 124, Berlin, 2006.
[10] C. Bohren, D. Huffman, Absorption and Scattering of Light by Small Particles, Wiley, New York, 1983.
[11] K. Larson-Smith, A. Jackson, D.C. Pozzo, J. Colloid Interface Sci. 343 (2010) 36.
[12] H. Kaya, Appl. Phys. A 74 (2002) S507.
[13] T. Fultterer, G.A. Vliegenthart, P.R. Lang, Macromolecules 37 (2004) 8407.
[14] P. Pusey, in: P. Lindner, T. Zemb (Eds.), Neutrons, X-rays and Light scattering Methods Applied to Soft Condensed Matter, Elsevier Science, Amsterdam, 2002, p. 3.
[15] S.J. Henderson, Biophys. J. 70 (1996) 1618.
[16] V.N. Manoharan, M.T. Elsesser, D.J. Pine, Science 301 (2003) 483.